circBIRC6 contributes to the development of non-small cell lung cancer via regulating microRNA-217/amyloid beta precursor protein binding protein 2 axis

Da Ni, Jiping Teng, Youshuang Cheng, Zhijun Zhu, Bufeng Zhuang, Zhiyin Yang

Department of Thoracic Surgery, Shanghai Ninth People's Hospital, Shanghai Jiao Tong University School of Medicine, Shanghai 201999, China.

Abstract

Background: Circular RNAs (circRNAs) are considered to be important regulators in cancer biology. In this study, we focused on the effect of circRNA baculoviral inhibitor of apoptosis protein (IAP) repeat containing 6 (circBIRC6) on non-small cell lung cancer (NSCLC) progression.

Methods: The NSCLC and adjacent non-tumor tissues were collected at Shanghai Ninth People's Hospital. Quantitative real-time polymerase chain reaction was conducted for assessing the levels of circBIRC6, amyloid beta precursor protein binding protein 2 (APPBP2) messenger RNA (mRNA), baculoviral IAP repeat containing 6 mRNA (BIRC6), and microRNA-217 (miR-217). Western blot assay was adopted for measuring the protein levels of APPBP2, E-cadherin, N-cadherin, and vimentin. Colony formation assay, transwell assay, and flow cytometry analysis were utilized for evaluating cell colony formation, metastasis, and apoptosis. Dualluciferase reporter assay and RNA immunoprecipitation assay were carried out to determine the interaction between miR-217 and circBIRC6 and APPBP2 in NSCLC tissues. The murine xenograft model assay was used to investigate the function of circBIRC6 in tumor formation *in vivo*. Differences were analyzed via Student's *t* test or one-way analysis of variance. Pearson's correlation coefficient analysis was used to analyze linear correlation.

Results: CircBIRC6 was overexpressed in NSCLC tissues and cells. Knockdown of circBIRC6 repressed the colony formation and metastasis and facilitated apoptosis of NSCLC cells in *vitro* and restrained tumorigenesis *in vivo*. Mechanically, circBIRC6 functioned as miR-217 sponge to promote APPBP2 expression in NSCLC cells. MiR-217 inhibition rescued circBIRC6 knockdown-mediated effects on NSCLC cell colony formation, metastasis, and apoptosis. Overexpression of miR-217 inhibited the malignant phenotypes of NSCLC cells, while the effects were abrogated by elevating APPBP2.

Conclusion: CircBIRC6 aggravated NSCLC cell progression by elevating APPBP2 via sponging miR-217, which might provide a fresh perspective on NSCLC therapy.

Keywords: Non-small cell lung cancer; Circular RNA baculoviral inhibitor of apoptosis protein repeat containing 6; MicroRNA-217; Amyloid beta precursor protein binding protein 2

Introduction

Non-small cell lung cancer (NSCLC) is a common malignant tumor, accounting for 80% to 85% of lung cancer.[1,2] Although the early detection and treatment have made great progress, most of the NSCLC patients are diagnosed at the advanced stage, and the overall survival rate remains dismal.[3,4] Therefore, exploring the potential mechanism of the pathogenesis of NSCLC may offer a theoretical basis to improve the diagnosis and therapy for this disease.

Circular RNAs (circRNAs) are a large group of non-coding RNAs (ncRNAs) that are featured by single-strand, loop-closed structures.[5] The discovery of circRNAs in cancer progression has broadened our insights into cancer pathogenesis.[6,7] Moreover, multiple studies suggested that circRNAs were aberrantly expressed in NSCLC and play crucial roles in the carcinogenesis of NSCLC. For example, circ_0003998 played an oncogenic role in NSCLC by regulating microRNA (miR)-326/Notch1 pathway.[8] Circ_0014130 aggravated NSCLC cell growth and restrained apoptosis by absorbing miR-142-5p and increasing insulin-like growth factor (IGF)-1.[9] Moreover, Yang *et al*[10] demonstrated the carcinogenesis of circRNA baculoviral inhibitor of apoptosis protein repeat containing 6 (circBIRC6) in NSCLC. Even so, the exact roles and related mechanisms in NSCLC still need to be explored.

Access this article online

Quick Response Code:

Website: www.cmj.org

DOI: 10.1097/CM9.0000000000001940

Correspondence to: Dr. Zhiyin Yang, Department of Thoracic Surgery, Shanghai Ninth People's Hospital, Shanghai Jiao Tong University School of Medicine, No. 280 Mohe Road, Baoshan District, Shanghai 201999, China
E-Mail: Jy611315@163.com

Chinese Medical Journal 2022;135(6)

Received: 07-06-2021; **Online:** 20-02-2022 **Edited by:** Peifang Wei

MicroRNAs (miRNAs) are small ncRNAs and participate in the occurrence and progression of cancers, including NSCLC. For instance, miR-665,[11] miR-1296,[12] and miR-425[13] serve as a promoter or suppressor in NSCLC progression via influencing cell growth, apoptosis, and metastasis. It has been widely accepted that circRNAs serve as the molecular sponges for miRNAs, which can influence gene expression through interacting with the 3′ untranslated region (3′UTR) of target messenger RNAs (mRNAs).[14,15] The circRNA/miRNA/mRNA regulatory axis has been gradually identified in NSCLC.[16-18] In this study, miR-217 was predicted to share the binding sites of circBIRC6 and amyloid beta precursor protein binding protein 2 (APPBP2). However, the relationships among circBIRC6, miR-217, and APPBP2 in NSCLC development have not been elucidated.

In the present research, we focused on exploring how circBIRC6 regulated NSCLC progression and then investigating the interactions among circBIRC6, miR-217, and APPBP2 in NSCLC development, which might contribute to the diagnosis and treatment of NSCLC.

Methods

Tissues acquisition

Thirty-six pairs of NSCLC tissue specimens and adjacent non-tumor tissue specimens were collected from NSCLC patients (22 males and 14 females; age, 46–81 years) at Shanghai Ninth People's Hospital during July 2014 and June 2018. The obtained specimens were stored at –80°C before use. The collection of samples was done after approval was obtained from the Ethics Committee of Shanghai Ninth People's Hospital and written informed consent forms were provided by the patients.

Cell culture

Human bronchial epithelial cell line (16HBE) and NSCLC cell lines (A549 and H1299) were obtained from Procell (Wuhan, China). H125 cell line was bought from Mingzhoubio (Ningbo, China). The PC-9 cell line was purchased from BNBIO (Beijing, China). These cells were maintained in Roswell Park Memorial Institute 1640 Medium (Procell) mixed with 10% fetal bovine serum (FBS; Procell) and 1% penicillin-streptomycin (Procell) at 37°C in a humid incubator with 5% CO_2.

RNA isolation, RNase R treatment, and quantitative real-time polymerase chain reaction (qRT-PCR) assay

Total RNA was obtained utilizing TRIzol (Invitrogen, Carlsbad, CA, USA). For RNase R treatment, total RNA was treated with or without 3 U/μg RNase R (Epicenter Biotechnologies, Madison, WI, USA) for 20 min at 37°C. Next, PrimeScript™ reverse transcription (RT) reagent Kit (Takara, Dalian, China) or TaqMan miRNA assays (Applied Biosystems, Carlsbad, CA, USA) was employed to reversely transcribe RNA into complementary DNAs (cDNAs). After that, the qRT-PCR assay was executed on the StepOnePlus Real-Time PCR System (Applied Biosystems) utilizing Synergy Brands, Inc. (SYBR) Premix Ex Taq II (Takara) and specific primers. The related primers were: circBIRC6: (F: 5′-CCACAGATACAAGTGACACTGC-3′ and R: 5′-CTGGAGTTTGCAGAGCAGTG-3′); BIRC6: (F: 5′-GCACGCGGAACGTCGAT-3′ and R: 5′-AACTGTGGCCCACTTAGCAAC-3′); miR-217: (F: 5′-TCGGCAGGTACTGCATCAGGAA-3′ and R: 5′-CTCAACTGGTGTCGTGGA-3′); APPBP2: (F: 5′-CGCTGTCGTGGACAACTACAT-3′ and R: 5′-ATAAGCGTCCCTGTTGGTAAAG-3′); U6: (F: 5′-CTCGCTTCGGCAGCACA-3′ and R: 5′-AACGCTTCACGAATTTGCGT-3′); glyceraldehyde 3-phosphate dehydrogenase (GAPDH): (F: 5′-GAAGGTGAAGGTCGGAGTC-3′ and R: 5′-GAAGATGGTGATGGGATTTC-3′). The expression was estimated via the $2^{-\Delta\Delta Ct}$ strategy with GAPDH or U6 as a negative control.

Western blot assay

Total protein was extracted with radioimmunoprecipitation assay buffer (Sigma-Aldrich, St. Louis, MO, USA) and quantified with bicinchoninic acid protein assay kit (Tiangen, Beijing, China). Following separation by sodium dodecyl sulfonate-polyacrylamide gel (Solarbio, Beijing, China) electrophoresis, the proteins were blotted to polyvinylidene difluoride membranes (Sigma-Aldrich). After that, the membranes were blocked for 1 h with 5% non-fat milk and cultivated overnight with primary antibodies against APPBP2 (bs-11639R; Bioss, Beijing, China), Vimentin (bs-0756R; Bioss), E-cadherin (bs-1519R; Bioss), N-cadherin (bs-1172R; Bioss), and GAPDH (bs-2188R; Bioss) at 4°C. Thereafter, the membranes were kept with horseradish peroxidase-conjugated secondary antibody (bs-0294M-HRP; Bioss) for 2 h at indoor temperature. The immunoblots were visualized by using enhanced chemiluminescence reagent (Beyotime, Shanghai, China).

Subcellular fraction assay

The nuclear RNA and cytoplasmic RNA in A549 and H1299 cells were isolated through the usage of Cytoplasmic and Nuclear RNA Purification Kit (Norgen Biotek, Thorold, Canada) in accordance with the instructions. The levels of circBIRC6, GAPDH (control for cytoplasmic transcript), and U6 (control for nuclear transcript) in the cytoplasmic and nuclear fractions were measured by the aforementioned qRT-PCR analysis.

Cell transfection

CircBIRC6 small interfering RNAs (siRNA) (si-circBIRC6#1, si-circBIRC6#2, and si-circBIRC6#3) and related control (si-NC), the overexpression plasmid of circBIRC6 (circBIRC6) and corresponding control (pCD5-ciR), mimic of miR-217 (miR-217) and mimic control (miR-NC), inhibitor of miR-217 (in-miR-217) and inhibitor control (in-miR-NC), the overexpression plasmid of APPBP2 (APPBP2) and its control (pcDNA), circBIRC6 short hairpin (sh) RNA (sh-circBIRC6) and its control sh-NC were synthesized by GenePharma (Shanghai, China). The compositions were transfected into A549 and H1299 cells utilizing Lipofectamine 2000 regent (Invitrogen).

Colony formation assay

After relevant transfection for 48 h, NSCLC cells (300 cells/well) were harvested and seeded into 6-well plates for colony formation. The media were changed every 3 days. After cultivation for 14 days, the colonies were dyed by adding 0.1% crystal violet (Solarbio) and imaged under a microscope. The colonies were counted if a clone contained > 50 cells.

Transwell assay

For cell migration determination, A549 and H1299 cells (2×10^4) with relevant transfection were suspended in 200 μL serum-free medium and inoculated into the upper compartments of transwell insert chambers (BD Bioscience, San Jose, CA, USA), while 600 μL medium mixed with 10% FBS (Procell) was filled into the bottom compartments. After 48 h, the cells on the top side of membranes were removed and the cells adhered to the lower surface were immersed in 4% paraformaldehyde (Sigma-Aldrich), dyed with 0.1% crystal violet (Solarbio) and then photographed and counted under an inverted microscope (Olympus, Tokyo, Japan) on the magnification of 100 ×. For cell invasion determination, the transwell insert chambers (BD Bioscience) precoated with Matrigel (Solarbio) were utilized and the other steps were consistent with the migration experiment.

Flow cytometry analysis

The Annexin V-fluorescein isothiocyanate (FITC)/propidium iodide (PI) Apoptosis Detection Kit (Beyotime) was employed for the analysis of cell apoptosis. In brief, NSCLC cells (1×10^5 cells/well) were plated onto 6-well plates and then incubated with 5 μL AnnexinV-FITC and 5 μL PI for 20 min in the dark according to the manufacturers' instructions. Thereafter, the cells were subjected to flow cytometry analysis (BD Biosciences, San Jose, CA, USA).

Prediction software

The relationships of circBIRC6, miR-217, and APPBP2 were analyzed by Starbase (https://starbase.sysu.edu.cn/) and Targetscan (http://www.targetscan.org/vert_72/).

Dual-luciferase reporter assay

The wild-type (WT) sequences of circBIRC6 and APPBP2 3′UTR containing the predicted binding sites of miR-217 were cloned into pmirGLO plasmid (Promega, Fitchburg, WI, USA), generating circBIRC6 WT and APPBP2 3′UTR-WT. Likewise, the mutant (MUT) sequences of circBIRC6 and APPBP2 3′UTR lacking miR-217 binding sequences were inserted into pmirGLO plasmid (Promega), generating circBIRC6 MUT and APPBP2 3′UTR-MUT. Then the generated plasmids were transfected into NSCLC cells together with miR-217 or miR-NC. 48 h post-transfection, the luciferase activity was determined with the Dual-Luciferase Reporter Assay Kit (Promega).

RNA immunoprecipitation (RIP) assay

RIP experiment was conducted utilizing the Magna RIP RNA-Binding Protein Immunoprecipitation Kit (Millipore, Billerica, MA, USA). Briefly, A549 and H1299 cells were diluted in RIP buffer and maintained with Anti-Immunoglobulin G (Anti-IgG) or Anti-argonaute 2 (anti-Ago2) (Abcam, Cambridge, MA, USA; Anti-Ago2 was used to detect Ago2, and then Ago2-RIP could be used to analyze the amount of circRNA and mRNA bound by miRNA) for 3 h. Then, the RNA in the immunoprecipitates was isolated and subjected to qRT-PCR as mentioned above.

Murine xenograft model

The animal study was approved by the Ethics Committee of Animal Research of Shanghai Ninth People's Hospital. The BALB/C nude mice were obtained from Beijing Vital River Laboratory Animal Technology Co., Ltd. (Beijing, China). sh-NC or sh-circBIRC6 transfected A549 cells were prepared as cell suspension and subcutaneously inoculated into the nude mice. After that, tumor volume was determined every 5 days and estimated with the equation: volume (mm^3) = length × width^2 × 0.5. On day 30, the mice were sacrificed and then tumors were weighed and preserved at –80°C until use.

Statistical analysis

The experiments were conducted triple times. All data were estimated with GraphPad Prism 7 (GraphPad Inc., La Jolla, CA, USA) and presented as mean ± standard deviation. Differences were compared with Student's t test or one-way analysis of variance. Pearson's correlation coefficient analysis was employed for the correlations among the levels of circBIRC6, miR-217, and APPBP2 in NSCLC tissues. P value < 0.05 was considered to be statistically significant.

Results

CircBIRC6 and APPBP2 were upregulated in NSCLC tissues and cells

In the beginning, the expression of circBIRC6 in NSCLC tissues and adjacent normal tissues was detected by qRT-PCR assay, which showed that circBIRC6 was drastically elevated in NSCLC tissues in comparison with normal tissues (11.070 ± 4.388 *vs.* 0.979 ± 0.343, $P < 0.001$) [Figure 1A]. Likewise, circBIRC6 level was notably elevated in NSCLC cells (H125, PC-9, A549, and H1299) as compared with 16HBE cells (all $P < 0.05$) [Figure 1B]. In view of the higher expression of circBIRC6 in A549 and H1299 cells than in H125 and PC-9 cells, A549 and H1299 cells were used for the subsequent experiments. In addition, the mRNA and protein levels of APPBP2 were enhanced in NSCLC tissues compared with adjacent normal tissues [Figure 1C and 1D]. Moreover, the results of qRT-PCR assay and western blot assay exhibited that APPBP2 mRNA and protein levels were all increased in A549 and H1299 cells compared with 16HBE cells [Figure 1E and 1F]. These results indicated that circBIRC6 and APPBP2 might be involved in NSCLC progression.

CircBIRC6 knockdown inhibited cell colony formation, migration, and invasion, but promoted apoptosis in NSCLC cells

As shown in Figure 2A and 2B, circBIRC6 was resistant to RNase R treatment, while linear BIRC6 was markedly

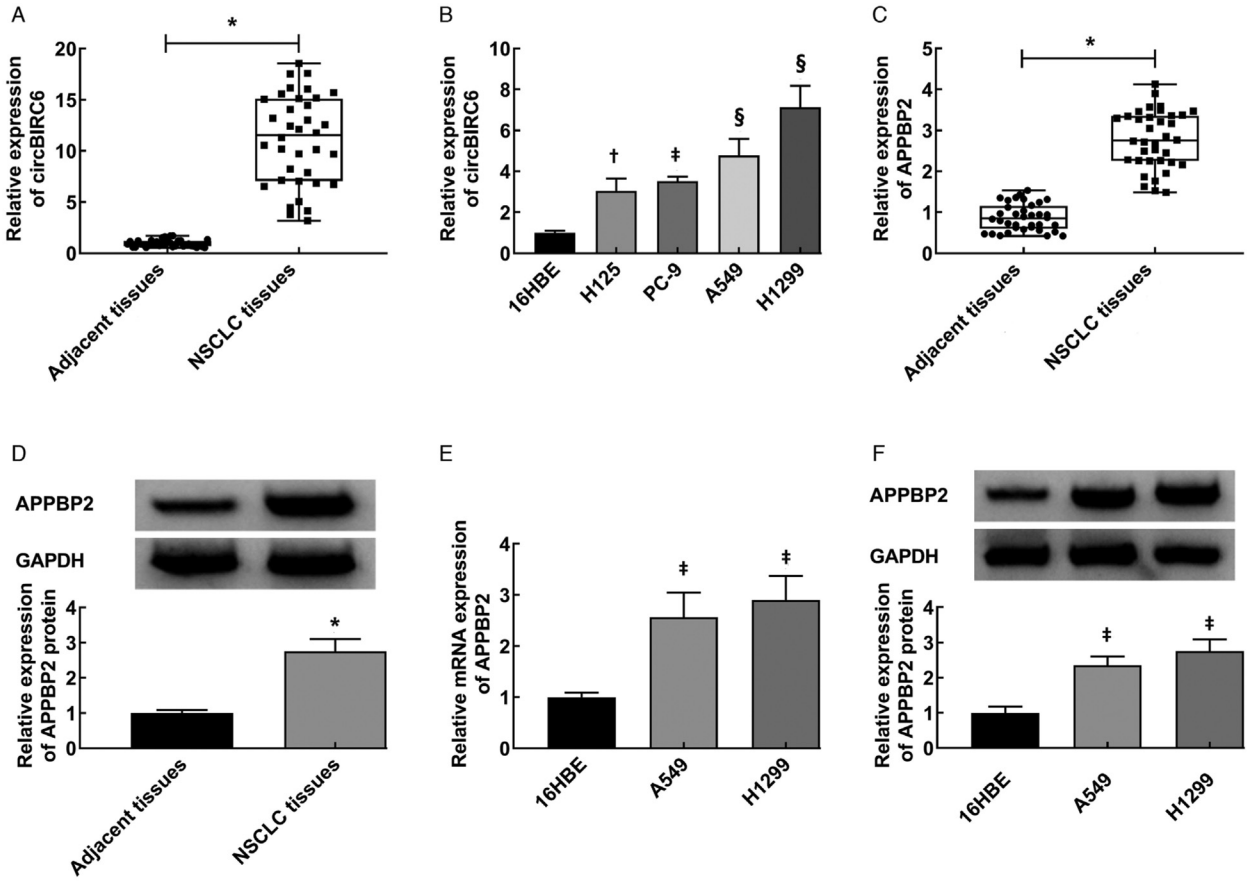

Figure 1: High expression of circBIRC6 and APPBP2 in NSCLC tissues and cells. (A) The expression of circBIRC6 in NSCLC tissues ($n = 36$) and adjacent non-tumor tissues ($n = 36$) was determined via qRT-PCR assay. (B) The expression of circBIRC6 in 16HBE, H125, PC-9, A549, and H1299 cells was examined through qRT-PCR assay. (C, D) The mRNA and protein levels of APPBP2 in NSCLC tissues and normal tissues were measured by qRT-PCR assay and western blot assay, respectively. (E, F) The mRNA and protein levels of APPBP2 in 16HBE, A549, and H1299 cells were detected through qRT-PCR assay and western blot assay, respectively. $^{*}P < 0.05$, *vs.* adjacent tissues. $^{\dagger}P < 0.05$, $^{\ddagger}P < 0.01$, $^{\S}P < 0.001$, *vs.* 16HBE. APPBP2: Amyloid beta precursor protein binding protein 2; circBIRC6: Circular RNA baculoviral inhibitor of apoptosis protein (IAP) repeat containing 6; GAPDH: Glyceraldehyde 3-phosphate dehydrogenase; mRNA: Messenger RNA; NSCLC: Non-small cell lung cancer; qRT-PCR: Quantitative real-time polymerase chain reaction; 16HBE: Human bronchial epithelial cell line.

digested by RNase R treatment, indicating that circBIRC6 was stable. Subcellular fraction assay indicated that circBIRC6 was mainly enriched in the cytoplasm of A549 and H1299 cells [Figure 2C and 2D]. Subsequently, to investigate the functional roles of circBIRC6 in NSCLC development, si-circBIRC6#1, si-circBIRC6#2, or si-circBIRC6#3 was transfected into A549 and H1299 cells. The transfection efficiency was assessed by qRT-PCR assay, which showed the transfection efficiency of si-circBIRC6#3 was better than si-circBIRC6#1 and si-circBIRC6#2 [Figure 2E and 2F]. Thus, si-circBIRC6#3 was used for further functional experiments. Colony formation assay presented that colony numbers of A549 and H1299 cells were evidently reduced after the deficiency of circBIRC6 compared with control groups [Figure 2G]. As demonstrated by the transwell assay, the migration and invasion abilities of A549 and H1299 cells were apparently repressed by silencing circBIRC6 [Figure 2H and 2I]. Moreover, flow cytometry analysis showed that circBIRC6 knockdown distinctly induced the apoptosis of A549 and H1299 cells compared with si-NC groups [Figure 2J]. In addition, the protein levels of epithelial-mesenchymal transition (EMT)-related markers in the transfected A549 and H1299 cells were measured via western blot assay. The results exhibited that circBIRC6 silencing remarkably increased E-cadherin level and evidently decreased N-cadherin and vimentin levels in both A549 and H1299 cells compared with si-NC groups [Figure 2K]. Collectively, circBIRC6 knockdown ameliorated the malignant behaviors of NSCLC cells.

CircBIRC6 directly bound to miR-217 to regulate NSCLC cell malignant behaviors

To verify the underlying mechanism of circBIRC6 in NSCLC cell progression, online website starBase was used to analyze the potential miRNAs of circBIRC6. As a result, miR-217 was found to be a target miRNA of circBIRC6 and their complementary sequences were shown in Figure 3A. Then dual-luciferase reporter assay was conducted to verify this prediction, presenting that miR-217 transfection prominently reduced the luciferase activity of circBIRC6 WT in A549 and H1299 cells, while the luciferase activity of circBIRC6 MUT was not affected by miR-217 transfection [Figure 3B]. RIP assay further proved the interaction between circBIRC6 and miR-217 because the enrichment of circBIRC6 and miR-217 was increased by Anti-Ago2 compared with Anti-IgG groups [Figure 3C]. Afterward,

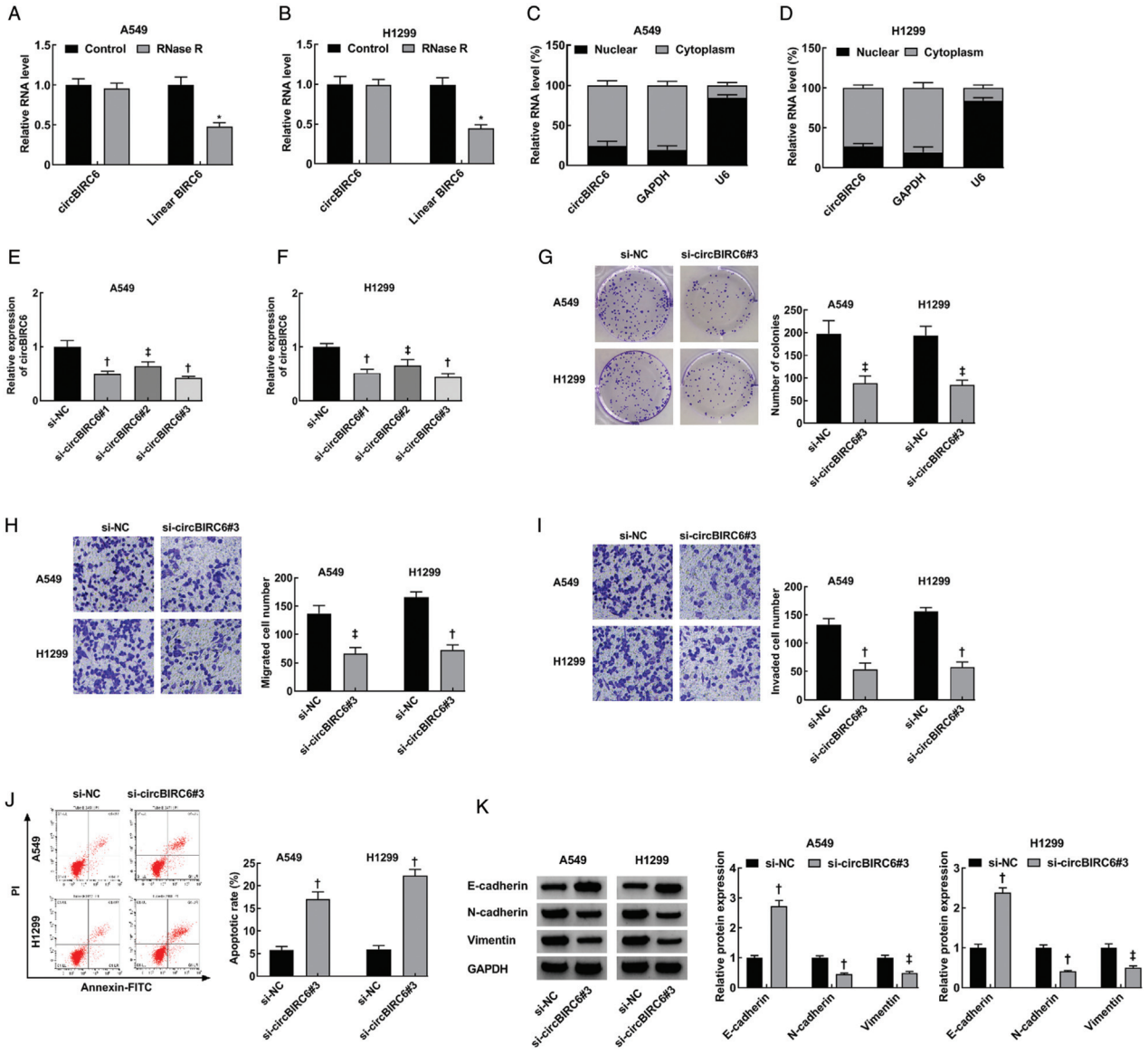

Figure 2: Effects of circBIRC6 knockdown on NSCLC cell colony formation, migration, Invasion, and apoptosis. (A, B) After total RNA In A549 and H1299 cells was treated with or without RNase R, the expression levels of circBIRC6 and BIRC6 were detected by qRT-PCR assay. (C, D) The relative expression of circBIRC6 in the nucleus and cytoplasm of A549 and H1299 cells was examined by qRT-PCR assay. (E, F) The expression of circBIRC6 in si-NC, si-circBIRC6#1, si-circBIRC6#2, or si-circBIRC6#3 transfected A549 and H1299 cells was determined by qRT-PCR assay. (G-K) A549 and H1299 cells were transfected with si-NC or si-circBIRC6#3. (G) The colony formation, (H, I) migration and invasion, and (J) apoptosis of A549 and H1299 cells were evaluated with colony formation assay, transwell assay, and flow cytometry analysis, respectively. (K) The protein levels of E-cadherin, N-cadherin, and vimentin in the transfected A549 and H1299 cells were measured via western blot assay. $^{*}P < 0.001$, *vs.* control. $^{\dagger}P < 0.001$, $^{\ddagger}P < 0.01$, *vs.* si-NC. circBIRC6: Circular RNA baculoviral inhibitor of apoptosis protein (IAP) repeat containing 6; FITC: Fluorescein isothiocyanate; GAPDH: Glyceraldehyde 3-phosphate dehydrogenase; NC: Negative control; NSCLC: Non-small cell lung cancer; PI: Propidium iodide; qRT-PCR: Quantitative real-time polymerase chain reaction; si: Small interfering.

the qRT-PCR assay showed that miR-217 was lowly expressed in NSCLC tissues and cells compared with normal tissues and cells [Figure 3D and 3E]. Subsequently, circBIRC6 was successfully transfected into A549 and H1299 cells, as demonstrated by its marked elevation in A549 and H1299 cells after circBIRC6 transfection [Figure 3F]. Furthermore, our results indicated that circBIRC6 overexpression dramatically reduced miR-217 level in A549 and H1299 cells, while circBIRC6 knockdown led to an opposite outcome [Figure 3G]. To summarize, circBIRC6 sponged miR-217 to negatively modulate miR-217 expression in NSCLC cells.

As presented in Figure 3H, the transfection of in-miR-217 led to a remarkable reduction of miR-217 level in A549 and H1299 cells compared with in-miR-NC transfected groups. Subsequently, A549 and H1299 cells were treated with si-NC, si-circBIRC6#3, si-circBIRC6#3+in-miR-NC, or si-circBIRC6#3+in-miR-217 to explore the association between circBIRC6 and miR-217 in the regulation of NSCLC cell progression. The qRT-PCR assay showed that si-circBIRC6#3 transfection notably upregulated miR-217 expression in both A549 and H1299 cells, while the effect was rescued by in-miR-217 transfection [Figure 3I and 3J]. As illustrated by colony formation assay, transwell assay,

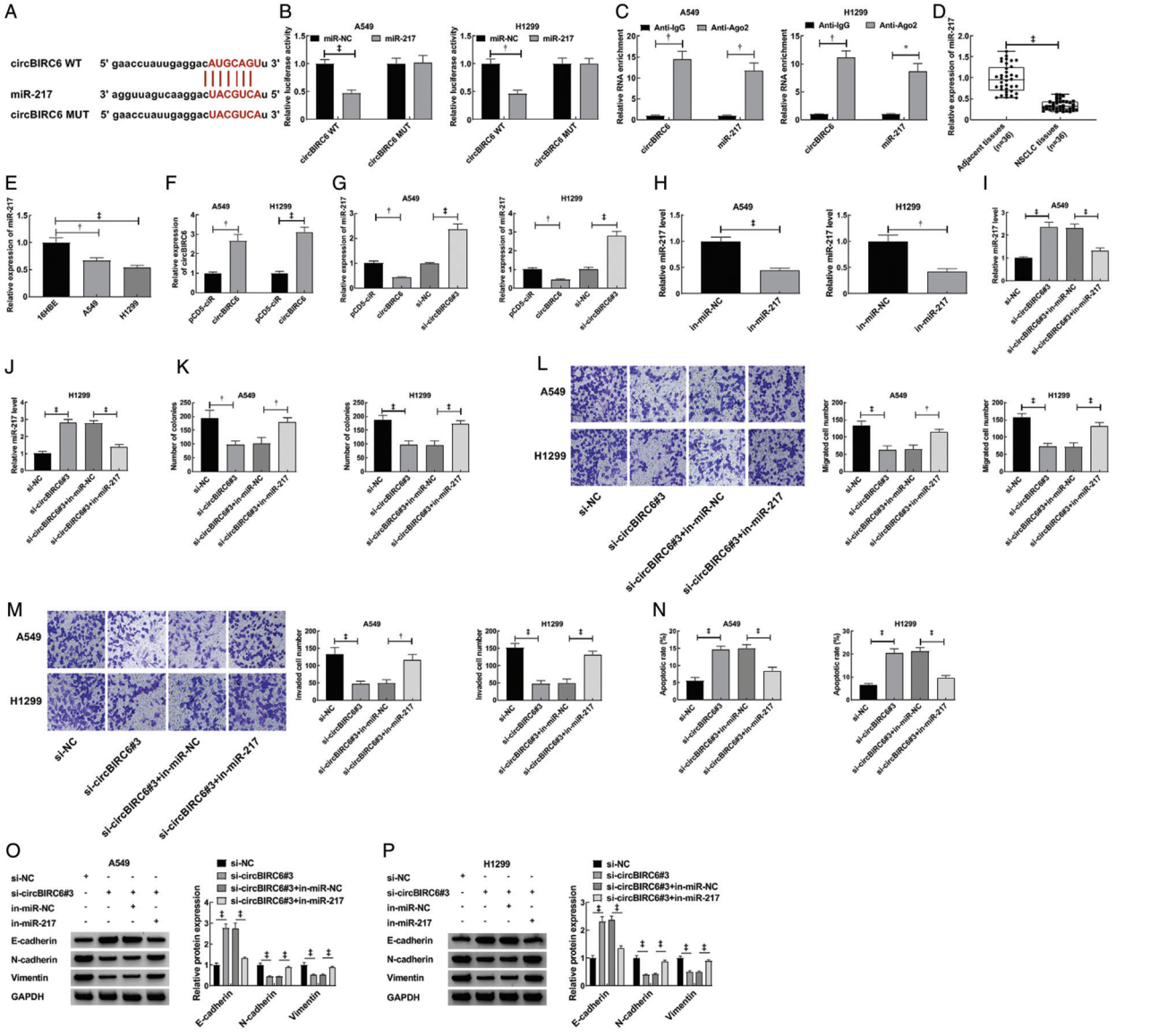

Figure 3: CircBIRC6 knockdown inhibited the malignant behaviors of NSCLC cells by targeting miR-217. (A) The binding sites between circBIRC6 and miR-217. (B) The luciferase activity in A549 and H1299 cells co-transfected with miR-NC/miR-217 and circBIRC6 WT/circBIRC6 MUT was measured by dual-luciferase reporter assay. (C) After RIP assay was carried out with anti-IgG or anti-Ago2, the enrichment of circBIRC6 and miR-217 was examined with qRT-PCR assay. (D, E) The expression of miR-217 in NSCLC tissues, cells and matched normal tissues and cells was detected by qRT-PCR assay. (F) The expression level of circBIRC6 in A549 and H1299 cells transfected with pCD5-ciR or circBIRC6 was measured by qRT-PCR assay. (G) After A549 and H1299 cells were transfected with pCD5-ciR, circBIRC6, si-NC, or si-circBIRC6#3, the expression of miR-217 was detected by qRT-PCR assay. (H) The expression of miR-217 in A549 and H1299 cells transfected with in-miR-NC or in-miR-217 was determined by qRT-PCR assay. (I-P) A549 and H1299 cells were transfected with si-NC, si-circBIRC6#3, si-circBIRC6#3+in-miR-NC, or si-circBIRC6#3+in-miR-217. (I, J) The level of miR-217 in the transfected A549 and H1299 cells was determined through qRT-PCR assay. (K) Cell colony formation, (L, M) migration and invasion, and (N) apoptosis in A549 and H1299 cells were evaluated by colony formation assay, transwell assay, and flow cytometry analysis, respectively. (O, P) The protein levels of E-cadherin, N-cadherin, and vimentin in A549 and H1299 cells were measured via western blot assay. $^{*}P < 0.05$, $^{\dagger}P < 0.01$, $^{\ddagger}P < 0.001$. Anti-Ago2: Anti-argonaute 2; Anti-IgG: Anti-immunoglobulin G; ciR: Circular RNA; circBIRC6: Circular RNA baculoviral inhibitor of apoptosis protein (IAP) repeat containing 6; GAPDH: Glyceraldehyde 3-phosphate dehydrogenase; in-miR-217: Inhibitor of miR-217; in-miR-NC: Inhibitor control; miR: MicroRNA; miR-NC: Negative control of miR-217 mimics; MUT: Mutant; NSCLC: Non-small cell lung cancer; qRT-PCR: Quantitative real-time polymerase chain reaction; 3′UTR: Untranslated region; RIP: RNA immunoprecipitation; si-circBIRC6: Small interfering RNA of circular RNA baculoviral IAP repeat containing 6; si-NC: Negative control of circBIRC6 small interfering RNA; WT: Wild-type.

and flow cytometry assay, the inhibitory effects on NSCLC cell colony formation, migration and invasion, and the promotional effect on cell apoptosis mediated by circBIRC6 knockdown were all abrogated by downregulating miR-217 [Figure 3K-N]. Moreover, miR-217 inhibition ameliorated circBIRC6 knockdown-mediated promotion on E-cadherin level and suppression on N-cadherin and vimentin levels in A549 and H1299 cells [Figure 3O and 3P]. Based on these results, we concluded that circBIRC6 silencing restrained NSCLC cell growth and metastasis and induced apoptosis via sponging miR-217.

Overexpression of miR-217 suppressed the malignant phenotypes of NSCLC cells by targeting APPBP2

By analyzing bioinformatics prediction website Targetscan, APPBP2 was predicted to be a target gene of miR-217 and their potential binding sites were exhibited in

Figure 4A. To confirm this prediction, dual-luciferase reporter assay was carried out. The results showed that miR-217 transfection impeded the luciferase activity of APPBP2 3′UTR-WT in A549 and H1299 cells, but did not affect the luciferase activity of APPBP2 3′UTR-MUT [Figure 4B]. Then RIP assay was further conducted to verify the interaction between miR-217 and APPBP2, which showed that miR-217 and APPBP2 were markedly enriched in anti-Ago2 RIP groups compared with Anti-IgG RIP groups [Figure 4C]. Thereafter, miR-217 was successfully transfected into A549 and H1299 cells to elevate miR-217 expression [Figure 4D]. Moreover, our results indicated that miR-217 elevation conspicuously decreased APPBP2 protein level in A549 and H1299 cells, while miR-217 inhibition remarkably increased APPBP2 protein level in A549 and H1299 cells [Figure 4E]. All these results suggested that miR-217 could negatively regulate APPBP2 expression by targeting APPBP2.

As presented in Figure 4F, APPBP2 transfection caused a significant increase in APPBP2 protein level in A549 and H1299 cells compared with pcDNA groups. Next, A549 and H1299 cells were transfected with miR-NC, miR-217, miR-217 + pcDNA, or miR-217 + APPBP2 to explore the relationship between miR-217 and APPBP2 in NSCLC progression. The transfection efficiency was evaluated by western blot assay, exhibiting that miR-217 overexpression suppressed the protein level of APPBP2 in A549 and H1299 cells, while APPBP2 elevation reversed the impact [Figure 4G]. The results of colony formation assay indicated that miR-217 overexpression evidently inhibited the colony formation ability of A549 and H1299 cells, with APPBP2 upregulation reversing the effect [Figure 4H]. Transwell assay suggested that miR-217 overexpression restrained cell migration and invasion in both A549 and H1299 cells, while these effects were weakened by elevating APPBP2 [Figure 4I-K]. We also observed that miR-217 elevation facilitated the apoptosis of A549 and H1299 cells, while APPBP2 overexpression rescued the effect [Figure 4L]. In addition, we found that E-cadherin level was raised and N-cadherin and vimentin levels were declined in A549 and H1299 cells transfected with miR-217, whereas these effects were abolished after APPBP2 transfection [Figure 4M and 4N]. These results suggested that miR-217 overexpression hampered NSCLC cell colony formation and metastasis and induced apoptosis by binding to APPBP2.

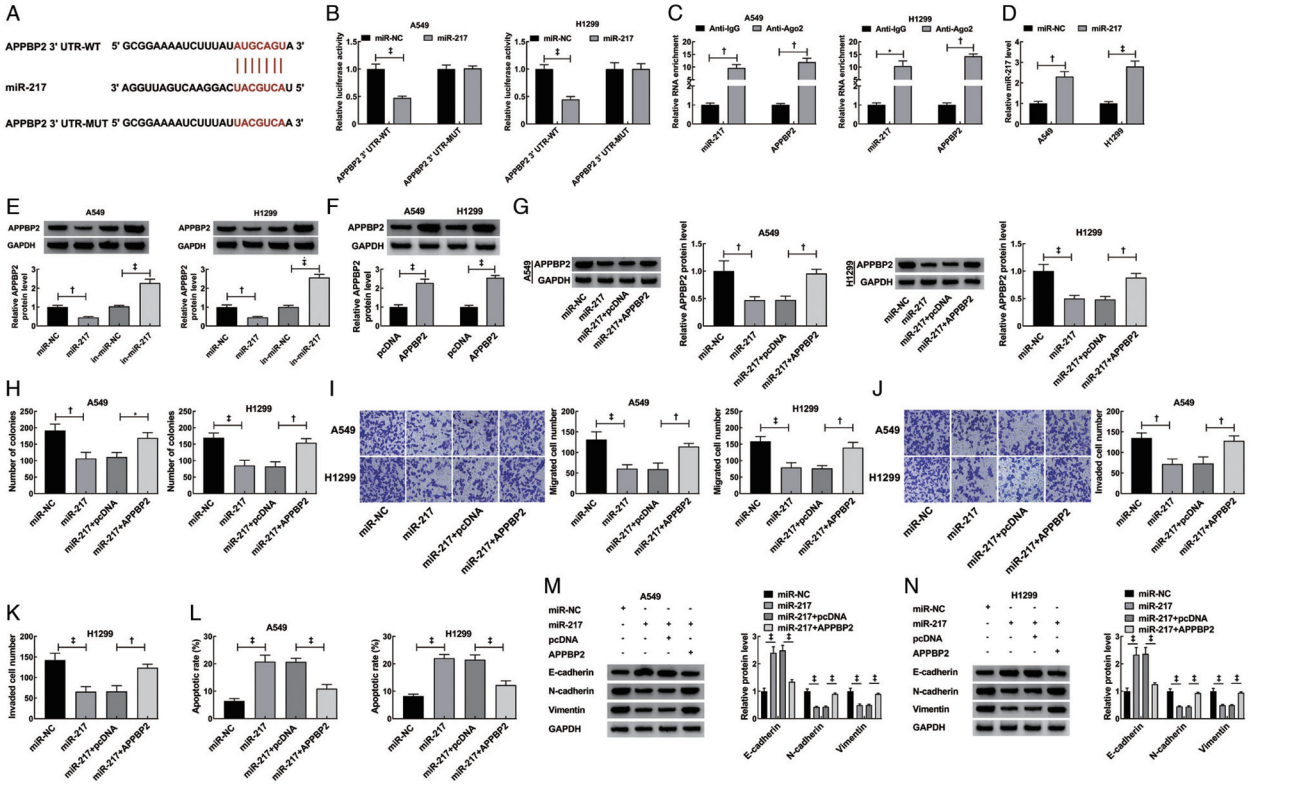

Figure 4: MiR-217 overexpression decelerated NSCLC progression by targeting APPBP2. (A) The binding sites between APPBP2 and miR-217. (B) The luciferase activity in A549 and H1299 cells transfected with miR-NC/miR-217 and APPBP2 3′UTR-WT/APPBP2 3′UTR-MUT was determined via dual-luciferase reporter assay. (C) The combination between miR-217 and APPBP2 was verified by RIP assay. (D) The expression of miR-217 in A549 and H1299 cells transfected with miR-NC or miR-217 was determined by qRT-PCR assay. (E) Following transfection of miR-NC, miR-217, in-miR-NC, or in-miR-217, the protein level of APPBP2 in A549 and H1299 cells was measured using western blot assay. (f) The protein level of APPBP2 in A549 and H1299 cells transfected with pcDNA or APPBP2 was measured by western blot assay. (G-N) A549 and H1299 cells were transfected with miR-NC, miR-217, miR-217 + pcDNA, or miR-217 + APPBP2. (G) The protein level of APPBP2 in A549 and H1299 cells was examined with western blot assay. (H) The colony formation, (I-K) migration and invasion, and (L) apoptosis in A549 and H1299 cells were analyzed by colony formation assay, transwell assay, and flow cytometry assay, respectively. (M, N) The protein levels of E-cadherin, N-cadherin, and vimentin in A549 and H1299 cells were examined via western blot assay. $^{*}P < 0.05$, $^{+}P < 0.01$, $^{\ddagger}P < 0.001$. Anti-Ago2: Anti-argonaute 2; Anti-IgG:Anti-immunoglobulin G; APPBP2: Amyloid beta precursor protein binding protein 2; GAPDH: Glyceraldehyde 3-phosphate dehydrogenase; in-miR-217: Inhibitors of miR-217; in-miR-NC: Negative control of miR-217 inhibitors; NSCLC: Non-small cell lung cancer; miR-217: MicroRNA-217; miR-NC: Negative control of miR-217 mimics; qRT-PCR: Quantitative real-time polymerase chain reaction; RIP: RNA immunoprecipitation; 3′UTR-MUT: 3′Untranslated region mutant; 3′UTR-WT: 3′Untranslated region wild-type.

CircBIRC6 positively regulated APPBP2 expression via sponging miR-217

The relationships among circBIRC6, miR-217, and APPBP2 were investigated. As estimated by Pearson's correlation coefficient analysis, miR-217 level in NSCLC tissues was negatively correlated with circBIRC6 level and APPBP2 mRNA level [Figure 5A and 5B] (P = 0.0012 and 0.0077, respectively). Moreover, circBIRC6 level was positively correlated with APPBP2 mRNA level in NSCLC tissues [Figure 5C; $P < 0.0001$]. Additionally, our results indicated that circBIRC6 silencing markedly decreased the protein level of APPBP2 in A549 and H1299 cells, while miR-217 inhibition reversed the effect [Figure 5D-F]. These results suggested that circBIRC6 positively regulated APPBP2 expression via acting as miR-217 sponge.

CircBIRC6 knockdown inhibited tumor formation in vivo

To explore the role of circBIRC6 in tumor growth of NSCLC *in vivo*, sh-circBIRC6-transfected A549 cells were injected into the nude mice. As exhibited in Figure 6A and 6B, circBIRC6 silencing evidently reduced tumor volume at 20 ($P = 0.006$), 25 ($P < 0.001$) and 30 days ($P < 0.001$) and tumor weight ($P < 0.001$) compared with sh-NC groups. Then the tumors were harvested from the mice followed by determination for the levels of circBIRC6, miR-217, and APPBP2. The results showed that circBIRC6, APPBP2 mRNA, and APPBP2 protein levels were all declined and miR-217 level was enhanced in the tumors harvested from sh-circBIRC6 groups compared with sh-NC control groups [Figure 6C and 6D]. All these findings illustrated that circBIRC6 knockdown repressed tumor growth in vivo.

Discussion

With the development of RNA sequencing technology and bioinformatic analysis, multiple circRNAs have been discovered and researchers have focused on their impacts on tumor progression.[19] Up to date, the understandings of circRNAs on cancer development are still very limited. In this paper, we aimed to explore the effect of circBIRC6 on NSCLC progression. We found a distinct upregulation of circBIRC6 in NSCLC. Moreover, we demonstrated that circBIRC6 accelerated NSCLC malignancy through regulating circBIRC6/miR-217/APPBP2 axis.

CircRNAs function as vital modulators in the pathology and progression of NSCLC. For example, circ_101239 aggravated NSCLC development[20]; circRNA insulin like growth factor 1 receptor restrained the metastasis of

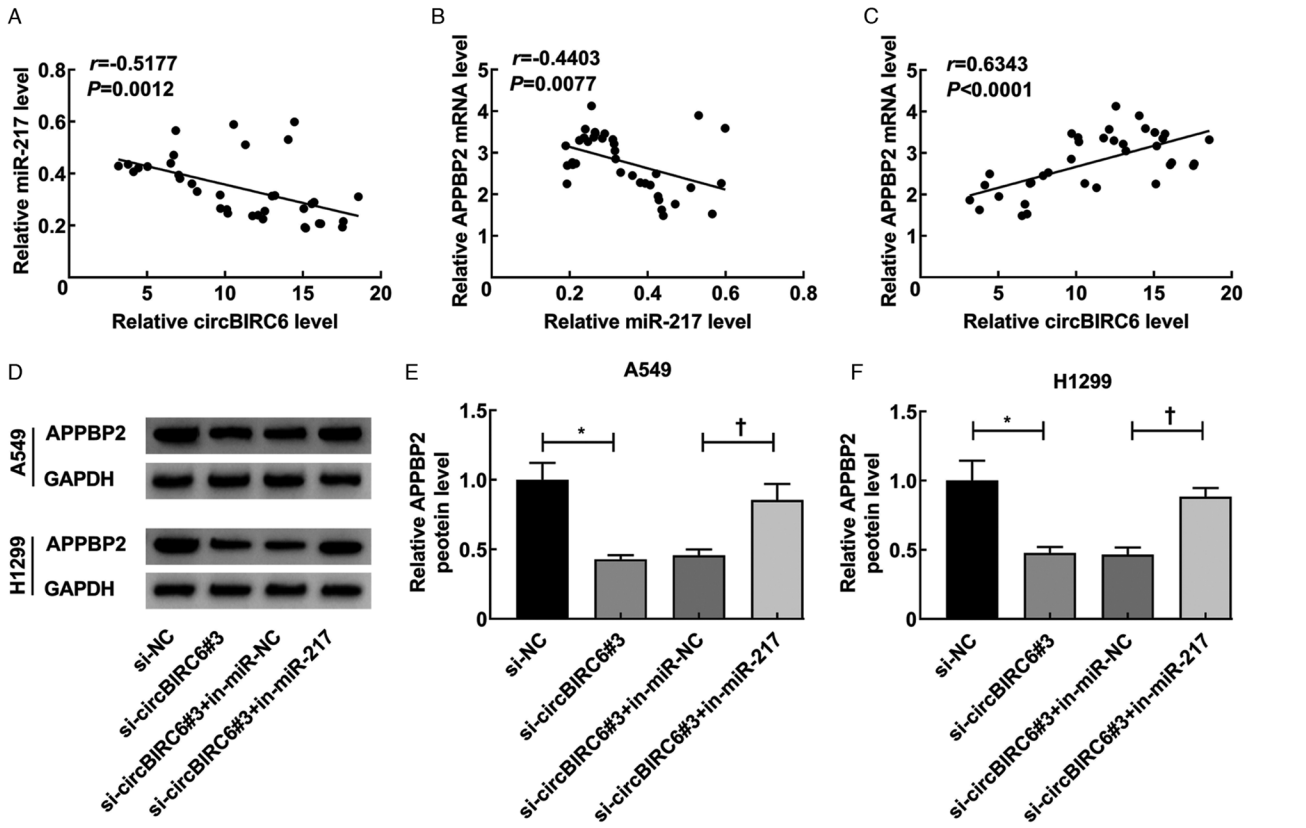

Figure 5: CircBIRC6 knockdown inhibited APPBP2 expression by targeting miR-217. (A-C) The correlations among the levels of circBIRC6, miR-217, and APPBP2 in NSCLC tissues ($n = 36$) were analyzed by Pearson's correlation coefficient analysis. (D-F) The protein level of APPBP2 in A549 and H1299 cells transfected with si-NC, si-circBIRC6#3, si-circBIRC6#3 + in-miR-NC, or si-circBIRC6#3 + in-miR-217 was measured by western blot assay. $^{*}P < 0.001$, $^{\dagger}P < 0.01$. APPBP2: Amyloid beta precursor protein binding protein 2; circBIRC6: Circular RNA baculoviral inhibitor of apoptosis protein (IAP) repeat containing 6; GAPDH: Glyceraldehyde 3-phosphate dehydrogenase; in-miR-217: Inhibitors of miR-217; in-miR-NC: Negative control of miR-217 inhibitors; miR-217: MicroRNA-217; mRNA: Messenger RNA; NSCLC: Non-small cell lung cancer; si-circBIRC6: Small interfering RNA of circular RNA baculoviral inhibitor of apoptosis protein (IAP) repeat containing 6; si-NC: Negative control of circBIRC6 small interfering RNA.

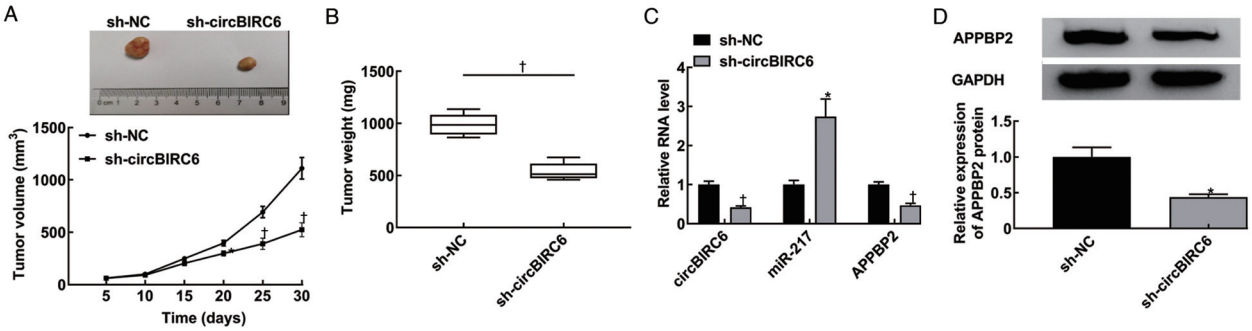

Figure 6: CircBIRC6 silencing blocked tumorigenesis *in vivo*. (A) Tumor volume was measured every 5 days. (B) Tumor weight was examined after 30 days. (C) The levels of circBIRC6, miR-217, and APPBP2 mRNA in the tumors were determined by qRT-PCR assay. (D) The protein level of APPBP2 in the tumors was measured via western blot assay. $^{*}P < 0.01$, $^{+}P < 0.001$, *vs.* sh-NC. APPBP2: Amyloid beta precursor protein binding protein 2; circBIRC6: Circular RNA baculoviral inhibitor of apoptosis protein (IAP) repeat containing 6; GAPDH: Glyceraldehyde 3-phosphate dehydrogenase; miR-217: MicroRNA-217; qRT-PCR: Quantitative real-time polymerase chain reaction; sh-NC: Negative control of circBIRC6 short hairpin RNA.

NSCLC[21]; circ_0020123 overexpression triggered NSCLC cell growth, migration and invasion, and impaired apoptosis.[22] Of note, Yang *et al*[10] declared that circBIRC6 was overexpressed in NSCLC and exerted onco[2]g[3]e]nic properties by acting as miR-145 sponge. Jin *etal*[23]revealed that circBIRC6silencing inhibited NSCLC cell proliferation and metastasis and repressed apoptosis via targeting miR-4491. In the present research, the function of circBIRC6 in NSCLC was further determined. CircBIRC6 was found to be highly expressed in NSCLC. Functionally, our results exhibited that circBIRC6 knockdown impaired cell colony formation and motility but triggered apoptosis in NSCLC cells. Moreover, we determined the effect of circBIRC6 on EMT process, which is a vital mechanism associated with metastasis, via examining the levels of EMT markers (E-cadherin, N-cadherin, and vimentin).[24] Prudkin *et al*[25] verified the reduction of E-cadherin and the elevation of N-cadherin and vimentin in lung cancer. In line with the previous results, we found that circBIRC6 deficiency enhanced E-cadherin and reduced N-cadherin and vimentin levels in NSCLC cells, indicating the inhibition of EMT process. In addition, we demonstrated that circBIRC6 facilitated tumor formation *in vivo*. Collectively, circBIRC6 played a tumor-promoting role in NSCLC.

Subsequently, the underlying mechanism of circBIRC6 in NSCLC malignancy was elucidated. Stepwise investigations indicated that miR-217 functioned as an intermediate bridge between circBIRC6 and APPBP2, that is, circBIRC6 could promote APPBP2 expression through sponging miR-217. Liu *et al*[26] unraveled that miR-217 level was declined in NSCLC tissues and participated in regulating NSCLC cell growth and motility via the circ_0023404/miR-217/ zinc finger E-box binding homeobox 1 axis. Chen *et al*[27] uncovered that miR-217 was weakly expressed in NSCLC cells and suppressed cell proliferation and metastasis via interacting with dachshund homolog 1. In line with these reports, we found that miR-217 level was diminished in NSCLC, and upregulation of miR-217 impeded NSCLC cell colony formation and motility and facilitated apoptosis. Moreover, circBIRC6 knockdown-mediated effect on NSCLC cell progression was ameliorated by the suppression of miR-217, hinting that circBIRC6 regulated NSCLC malignancy via absorbing miR-217. Additionally, we, for the first time, verified the interaction between miR-217 and APPBP2. APPBP2 was reported to accelerate NSCLC cell growth and motility.[28] Herein, our outcomes exhibited that APPBP2 elevation overturned the impacts of miR-217 overexpression in the malignant phenotypes of NSCLC cells, which suggested that miR-217 regulated NSCLC development via targeting APPBP2.

Altogether, circBIRC6 was abnormally elevated in NSCLC and played a carcinogenic role in NSCLC via absorbing miR-217 and increasing APPBP2. This study provided a novel avenue for seeking therapeutic targets of NSCLC.

Conflicts of interest

None.

References

1. Herbst RS, Morgensztern D, Boshoff C. The biology and management of non-small cell lung cancer. Nature 2018;553:446–454. doi: 10.1038/nature25183.
2. Bray F, Ferlay J, Soerjomataram I, Siegel RL, Torre LA, Jemal A. Global cancer statistics 2018: GLOBOCAN estimates of incidence and mortality worldwide for 36 cancers in 185 countries. CA Cancer J Clin 2018;68:394–424. doi: 10.3322/caac.21492.
3. Bareschino MA, Schettino C, Rossi A, Maione P, Sacco PC, Zeppa R, *et al*. Treatment of advanced non small cell lung cancer. J Thorac Dis 2011;3:122–133. doi: 10.3978/j.issn.2072-1439.2010.12.08.
4. Osmani L, Askin F, Gabrielson E, Li QK. Current WHO guidelines and the critical role of immunohistochemical markers in the subclassification of non-small cell lung carcinoma (NSCLC): moving from targeted therapy to immunotherapy. Semin Cancer Biol 2018;52:103–109. doi: 10.1016/j.semcancer.2017.11.019.
5. Chen LL. The biogenesis and emerging roles of circular RNAs. Nat Rev Mol Cell Biol 2016;17:205–211. doi: 10.1038/nrm.2015.32.
6. Zhao ZJ, Shen J. Circular RNA participates in the carcinogenesis and the malignant behavior of cancer. RNA Biol 2017;14:514–521. doi: 10.1080/15476286.2015.1122162.
7. Chen B, Huang S. Circular RNA: an emerging non-coding RNA as a regulator and biomarker in cancer. Cancer Lett 2018;418:41–50. doi: 10.1016/j.canlet.2018.01.011.
8. Yu W, Jiang H, Zhang H, Li J. Hsa_circ_0003998 promotes cell proliferation and invasion by targeting miR-326 in non-small cell lung cancer. Onco Targets Ther 2018;11:5569–5577. doi: 10.2147/OTT.S174750.
9. Wang M, Shi J, Jiang H, Xu K, Huang Z. Circ_0014130 participates in the proliferation and apoptosis of nonsmall cell lung cancer cells via the miR-142-5p/IGF-1 axis. Cancer Biother Radiopharm 2020;35:233–240. doi: 10.1089/cbr.2019.2965.
10. Yang H, Zhao M, Zhao L, Li P, Duan Y, Li G. CircRNA BIRC6 promotes non-small cell lung cancer cell progression by sponging microRNA-145. Cell Oncol (Dordr) 2020;43:477–488. doi: 10.1007/s13402-020-00503-x.

11. Xia J, Li D, Zhu X, Xia W, Qi Z, Li G, *et al*. Upregulated miR-665 expression independently predicts poor prognosis of lung cancer and facilitates tumor cell proliferation, migration and invasion. Oncol Lett 2020;19:3578–3586. doi: 10.3892/ol.2020.11457.
12. Deng H, Xie C, Ye Y, Du Z. MicroRNA-1296 expression is associated with prognosis and inhibits cell proliferation and invasion by Wnt signaling in non-small cell lung cancer. Oncol Lett 2020;19:623–630. doi: 10.3892/ol.2019.11154.
13. Jiang L, Ge W, Geng J. miR-425 regulates cell proliferation, migration and apoptosis by targeting AMPH-1 in non-small-cell lung cancer. Pathol Res Pract 2019;215:152705. doi: 10.1016/j.prp.2019.152705.
14. Kulcheski FR, Christoff AP, Margis R. Circular RNAs are miRNA sponges and can be used as a new class of biomarker. J Biotechnol 2016;238:42–51. doi: 10.1016/j.jbiotec.2016.09.011.
15. Liang ZZ, Guo C, Zou MM, Meng P, Zhang TT. circRNA-miRNA-mRNA regulatory network in human lung cancer: an update. Cancer Cell Int 2020;20:173. doi: 10.1186/s12935-020-01245-4.
16. Tan Z, Cao F, Jia B, Xia L. Circ_0072088 promotes the development of non-small cell lung cancer via the miR-377-5p/NOVA2 axis. Thorac Cancer 2020;11:2224–2236. doi: 10.1111/1759-7714.13529.
17. Chi Y, Luo Q, Song Y, Yang F, Wang Y, Jin M, *et al*. Circular RNA circPIP5K1A promotes non-small cell lung cancer proliferation and metastasis through miR-600/HIF-1alpha regulation. J Cell Biochem 2019;120:19019–19030. doi: 10.1002/jcb.29225.
18. An J, Shi H, Zhang N, Song S. Elevation of circular RNA circ_0003645 forecasts unfavorable prognosis and facilitates cell progression via miR-1179/TMEM14A pathway in non-small cell lung cancer. Biochem Biophys Res Commun 2019;511:921–925. doi: 10.1016/j.bbrc.2019.03.011.
19. Salzman J, Gawad C, Wang PL, Lacayo N, Brown PO. Circular RNAs are the predominant transcript isoform from hundreds of human genes in diverse cell types. PLoS One 2012;7:e30733. doi: 10.1371/journal.pone.0030733.
20. Zhang ZY, Gao XH, Ma MY, Zhao CL, Zhang YL, Guo SS. CircRNA_101237 promotes NSCLC progression via the miRNA-490-3p/MAPK1 axis. Sci Rep 2020;10:9024. doi: 10.1038/s41598-020-65920-2.
21. Xu Z, Xiang W, Chen W, Sun Y, Qin F, Wei J, *et al*. Circ-IGF1R inhibits cell invasion and migration in non-small cell lung cancer. Thorac Cancer 2020;11:875–887. doi: 10.1111/1759-7714.13329.
22. Wan J, Hao L, Zheng X, Li Z. Circular RNA circ_0020123 promotes non-small cell lung cancer progression by acting as a ceRNA for miR-488-3p to regulate ADAM9 expression. Biochem Biophys Res Commun 2019;515:303–309. doi: 10.1016/j.bbrc.2019.05.158.
23. Jin Z, Gao B, Gong Y, Guan L. Depletion of circ-BIRC6, a circular RNA, suppresses non-small cell lung cancer progression by targeting miR-4491. Biosci Trends 2021;14:399–407. doi: 10.5582/bst.2020.03310.
24. Thiery JP. Epithelial-mesenchymal transitions in development and pathologies. Curr Opin Cell Biol 2003;15:740–746. doi: 10.1016/j.ceb.2003.10.006.
25. Prudkin L, Liu DD, Ozburn NC, Sun M, Behrens C, Tang X, *et al*. Epithelial-to-mesenchymal transition in the development and progression of adenocarcinoma and squamous cell carcinoma of the lung. Mod Pathol 2009;22:668–678. doi: 10.1038/modpathol.2009.19.
26. Liu C, Zhang Z, Qi D. Circular RNA hsa_circ_0023404 promotes proliferation, migration and invasion in non-small cell lung cancer by regulating miR-217/ZEB1 axis. Onco Targets Ther 2019;12:6181–6189. doi: 10.2147/OTT.S201834.
27. Chen SS, Peng M, Zhou GZ, Pu YC, Yi MC, Zhu Y, *et al*. Long non-coding RNA HOTAIR regulates the development of non-small cell lung cancer through miR-217/DACH1 signaling pathway. Eur Rev Med Pharmacol Sci 2019;23:670–678. doi: 10.26355/eurrev_201901_16905.
28. Gong H, Liu F, Liu X, Min S, Wu N, Liu X, *et al*. APPBP2 enhances non-small cell lung cancer proliferation and invasiveness through regulating PPM1D and SPOP. EBioMedicine 2019;44:138–149. doi: 10.1016/j.ebiom.2019.05.028.

How to cite this article: Ni D, Teng J, Cheng Y, Zhu Z, Zhuang B, Yang Z. circBIRC6 contributes to the development of non-small cell lung cancer via regulating microRNA-217/amyloid beta precursor protein binding protein 2 axis. Chin Med J 2022;135:714–723. doi: 10.1097/CM9.0000000000001940